Structure of a-$Si_{1-x}C_x$:H alloys by wide-angle x-ray scattering: Detailed determination of first- and second-shell environment for Si and C atoms

C. Meneghini
Dipartimento di Fisica, Seconda Università di Roma, via della Ricerca Scientifica 1, Rome, Italy, and INFN, Laboratori Nazionali di Frascati, P.O. Box 13, 00044 Frascati, Rome, Italy

F. Boscherini
INFN, Laboratori Nazionali di Frascati, P.O. Box 13, 00044 Frascati, Rome, Italy

F. Evangelisti
Dipartimento di Fisica, Piazzale A. Moro 2, 00185 Rome, Italy

S. Mobilio
Dipartimento di Energetica, Università dell'Aquila, Roio Monteluco, 67100 L'Aquila, Italy and INFN, Laboratori Nazionali di Frascati, P.O. Box 13, 00044 Frascati, Rome, Italy
(Received 10 February 1994)

We present a study of the structure of a-$Si_{1-x}C_x$:H alloys by wide-angle x-ray scattering. By carefully analyzing the radial distribution functions and comparing with previous extended x-ray-absorption fine-structure measurements, we provide a detailed and quantitative description of local bonding around Si and C atoms. Among the results presented, most noteworthy are constant interatomic distances in first and second shells and the detection of a strong tendency for chemical order.

I. INTRODUCTION

The coexistence of topological and compositional disorder makes amorphous alloys very interesting from a fundamental point of view. Moreover, technological interest stems from the possibility of continuously changing sample characteristics and properties by varying the relative composition of constituent atoms. In a-$Si_{1-x}C_x$:H alloys the peculiarity of C atoms of having twofold, threefold, and fourfold coordination adds a degree of freedom to the local structural arrangement that is absent in other amorphous semiconductor alloys and makes it of particular interest and complexity. The complete exploitation of its promising technological properties is related to a full structural characterization. In fact many experimental and theoretical[1-28] studies have been performed to characterize a-$Si_{1-x}C_x$:H. Although the literature is sometimes contradictory, the following general picture emerges. a-$Si_{1-x}C_x$:H is a microscopically heterogeneous material in which four different phases can be present: a-$Si_{1-x}C_x$:H regions of predominant tetrahedral local structure, graphitic carbon (a Si-free microphase in which C is sp^2 hybridized), polymeric carbon (a Si-free microphase in which C makes polymeric chains of the type C_nH_{2n+m}), and voids.[15] The relative amount of each phase is very sensitive to the growth conditions. Notwithstanding its apparent oversimplification, it will be seen in the following that this "four-phase model" is extremely useful in the discussion of structural data.

Local structural determination in an amorphous binary alloy implies the measurement of (ideally all) bond lengths, bond angles, their mean-square fluctuation, the determination of the atomic identity of neighbors, and the measurements of the variation of these quantities with relative atomic concentration. As for the bond lengths, the questions to be addressed are whether there are variations in bond lengths and angles with respect to the crystalline case, the value of static disorder, and the possible variation of the quantities in a given sample series. In the case of a-$Si_{1-x}C_x$:H the particular type of bonding of C evidently adds a degree of freedom because of the presence of sp^3 and graphitic C configurations. We note that in Ge- and Si-based amorphous alloys average bond lengths have been determined to be equal to the value found in the corresponding crystal and not to vary appreciably with composition.[2,6,29-32] This situation must be compared with the situation in crystalline alloys, for example, pseudobinary alloys of the type $In_{1-x}Ga_xAs$.[33,34] In these compounds it has been found that individual bond lengths tend to remain close to the value found in the pure binary end member, with only a weak variation with composition.[35-38] The complete absence of this variation with composition in amorphous alloys seems to be a peculiarity of the amorphous state; it has been suggested recently that hydrogenation might contribute to this effect.[39]

The exact definition of the local atomic environment of the constituent elements (i.e., the chemical ordering of the alloy) is still an important question in both the experimental and theoretical literature. In principle, the relative disposition of the atoms on the network sites can vary between two very different situations: complete chemical order (CO), in which the elements are organized on network sites to maximize the number of heteronu-

 ©1994 The American Physical Society

clear bonds, and complete random order (RO), where all bonds have the same probability. It has been found[2] that CO is observed in covalent alloys in which the constituent atoms have a significant electronegativity difference (e.g., a-$Si_{1-x}N_x$:H and a-$Ge_{1-x}N_x$:H) while RO is found when the electronegativity difference is small (e.g., a-$Ge_{1-x}Si_x$:H and a-$Ge_{1-x}Sn_x$). This is related to the relative strength of the like and unlike bonds. The results of various structural studies on a-$Si_{1-x}C_x$:H have proposed different kinds of chemical order ranging from RO (Refs. 20 and 21) to near complete CO.[4,6,8,9,11,13-15]

Because of the particular structural features of a-$Si_{1-x}C_x$:H it is useful to comment on the determination of the type of chemical order present. In fact in an ideal continuous random network the presence and magnitude of homonuclear bonds for the minority atom is enough to distinguish between CO and RO. For a-$Si_{1-x}C_x$:H alloys the problem is more complex due to the special role played by C atoms, which can have different bonding configurations. Experimental data obtained with different spectroscopies[5,14,19-21] revealed that C-C bonds can be present also in Si-rich samples; this could be taken to imply the presence of RO. Nevertheless, an important experimental result is that the corresponding Si-Si homonuclear bonds are apparently absent in C-rich alloys,[6,13,17] which is clearly in contrast to the RO model and suggests a more complex picture in which C-C bonds are not homogeneously dispersed in the sample, but a separate Si-free microphase exists. In particular Petrich, Gleason, and Reimer[14] have suggested that higher hydrocarbons produced in the plasma phase could be incorporated in the samples during growth producing the observed C-C bonds in a polymer and/or graphite phase. Moreover, since the third-shell interatomic distance, which is 4.12 Å in diamond and 4.26 Å in graphite, matches the Si-Si second-shell distance of 3.85 Å better than that of C-C, which is about 2.5 Å, C clusters are apt to replace Si-Si bonds.[14,18]

Hydrogen inclusion plays a central role in the determination of the sample characteristics. Many studies have shown that it enhances heterocoordination,[5] it reduces stress and strain,[11,13,18] and promotes sp^3 over sp^2 C configurations.[16] Infrared[10] and NMR (Ref. 14) studies have shown that H is bonded preferably to sp^3 C in the CH_n configuration with $n=2,3$, whereas sp^2 C is non-hydrogenated and Si is at most monohydrogenated. This fact reduces the number of Si and C atoms which can be bonded to C. An important effect comes from the fact that the effective valence of C (defined for each atomic species as the difference between the total number of nearest neighbors and the number of H nearest neighbors) is less than that of Si: the stoichiometric concentration is shifted[12] at $x>0.5$.

Of great importance in structural studies is the comparison of experimental results with theoretical simulations. A complication in theoretical studies of a-$Si_{1-x}C_x$:H is the treatment of C bonds and phase separation effects. In fact the theoretical models proposed show dissimilarities. A continuous random network model[25] reproduces well the experimental bond distances, shows both sp^2 and sp^3 hybridizations on C sites, and presents a high degree of CO. On the other hand, the application of *ab initio* molecular-dynamics calculations on a-SiC produces a very disordered structure with a high degree of RO. The thermodynamical approach, represented by the free-energy model,[22,28,40] predicts a considerable amount of CO depending on H inclusion and on deposition temperature.

In order to gain further insight into these problems we have performed wide-angle x-ray-scattering (XRS) measurements of five samples of a-$Si_{1-x}C_x$:H, with x between 0.0 and 0.9. XRS yields the total radial distribution function (RDF) and thus yields a complete picture of local bonding, provided a careful analysis is performed in particular with regard to overlapping peaks. To this end a rigorous method[41] was applied to obtain quantitative structural information up to the second shell. The preliminary results have already been presented in a previous paper.[7] We also compare the present results with extended x-ray absorption fine-structure (EXAFS) ones[6] obtained by our group on samples grown in the same plasma-enhanced chemical-vapor deposition apparatus. EXAFS probes the local structure around Si and in the case of a-$Si_{1-x}C_x$:H the data showed a strong tendency for chemical order and that Si-Si and Si-C nearest-neighbor distances were constant with composition. In the framework of the four-phase model EXAFS probes the structure around Si in the alloys phase while XRS probes the total RDF. We believe that the complementary nature of the two techniques has allowed us to gain a very detailed picture of the local structure.

II. SAMPLE PREPARATION, EXPERIMENTAL APPARATUS, AND DATA HANDLING

The a-$Si_{1-x}C_x$:H samples were prepared by plasma-enhanced chemical-vapor deposition using a SiH_4 and CH_4 mixture at a substrate temperature of 110 °C. The total radio frequency power was between 15 and 20 W and the gas pressure was approximately 0.4 Torr. As the deposition rate of a-$Si_{1-x}C_x$:H decreases rapidly[10] with x, a substrate temperature lower than the standard was used. This permitted a sufficient quantity of material to be deposited, in particular for sample 5, for both XRS and concentration measurements with reasonable sample deposition times. The main sample characteristics are summarized in Table I.

For XRS measurements the samples were housed in holders in which the samples were contained between two Mylar windows in order to reduce absorption and scattering effects. XRS was performed using a diffractometer composed of a conventional Mo x-ray tube, a θ-2θ goniometer, and a NaI(Tl) detector. A quartz monochromator in the Johansson geometry was placed on the incident beam to remove the continuous spectrum and the K_β emission and to focus the beam. A voltage of 55 kV and a current of 40 mA were used to maximize the characteristic emission with respect to the bremsstrahlung background.[42,43] The symmetrical transmission geometry was used, as it is the best for small and weakly absorbing samples.[42,44] The x-ray source and receiving

TABLE I. Carbon concentrations and bulk density of samples studied.

Sample n	x	Bulk density (g/cm^3)
1	0.00	2.10
2	0.21	1.90
3	0.35	1.85
4	0.76	1.80
5	0.90	1.60

slits were placed on the Rowland circle of the crystal monochromator to realize the focusing geometry. Soller slit collimators were located between source and monochromator and between sample and receiving slits of the detector to reduce the axial beam divergence. For each sample data of different runs were averaged to minimize systematic errors. The acquisition time for each sample varied from 12 h for a-Si:H to 48 h for sample 5.

The sample concentration was measured by secondary neutral mass spectrometry (SNMS). A Leybold INA3 instrument was used[45] with an argon plasma as postionizer and a source of ions to sputter the samples. The negative voltage applied to the samples for sputtering was 1.2 keV and the primary current density was about 1–2 mA cm^{-2}. No charging problem occurred during the analysis even if SiC was known to be an insulating material. A stoichiometric SiC sample was used to obtain the relative sensitivity factor of C to Si at the analysis conditions used. Data quantification was performed using the INA3 data analysis program.

To extract the total structure factor (TSF) $i(q)$ from the experimental data we applied standard techniques,[42,44] which involve the removal of the parasitic scattering, the correction for absorption and polarization effects, the normalization to electron units, and the subtraction of the coherent independent scattering. The parasitic scattering includes the scattering of air and sample holder, the fluorescence contribution, and Compton and secondary scattering. The air and sample holder scattering was measured directly and subtracted, taking into account the effects of sample absorption. The Compton scattering was calculated using the theoretical values from Macgillavry and Rieck,[46] taking into account the Breit-Dirac recoil factor. Because of integration effects, secondary scattering, though partly coherent, does not contain any information about the structure. We have calculated the secondary scattering contribution according to Dwiggins.[47] It is greatest for the weakly absorbing (C-rich) samples, but it is always less than 5%. Moreover, as it is almost independent from q, in a first approximation it can be considered constant. The fluorescence contribution is incoherent and independent from q. Thus both the secondary scattering and the fluorescence were subtracted off as a constant value in the normalization procedure.[44] In order to transform the data from arbitrary units to e.u. we have used both the Krogh-Moe[48] and Norman[49] methods, yielding identical results.

Due to the width of the transmitted peak, experimental data started from $\theta \approx 3°$ ($q \approx 0.94$ Å^{-1}). We notice that experimental data exhibit a small-angle scattering tail which increases with x. This phenomenon can be related to an increasing microvoid density[12] and dishomogeneity.[8] The experimental data were extrapolated linearly from 0 to 1.2 Å^{-1} to reduce termination effects on the small-q side and to remove this small-angle scattering contribution. The bulk density was calculated by requiring that the total pair correlation functions (PCF's) were zero for distances less than the first real atomic distance in the sample.

III. DATA ANALYSIS

The experimental RDF is calculated from the TSF $i(q)$ using

$$J_{\text{exp}}(r)=4\pi r^2\rho(r)$$
$$=4\pi r^2\rho_0+\frac{2r}{\pi}\int_0^\infty qi(q)M(q)\sin(qr)dq\ , \tag{1}$$

with ρ_0 the mean atomic number density of the sample and $M(q)$ a modification function that essentially involves a Gaussian window, to reduce termination effects arising from finite range of experimental data, and a corrective term to compensate low-frequency oscillations in $i(q)$. We have used

$$M(q)=\frac{e^{-\alpha^2q^2}}{f_e^2} \tag{2}$$

with

$$f_e=\frac{\sum_i x_i f_i(q)}{\sum_i x_i f_i(0)} \tag{3}$$

the mean scattering factor per electron and x_i the concentration of the ith atomic species.

To extract structural information Eq. (1) is usually compared with a theoretical RDF $J_{\text{theo}}(r)$, in which position, width, and area of the peaks for each pair in each coordination shell are free parameters. Since an elementary fitting of the RDF with Gaussian contributions can be misleading in the presence of overlapping peaks and the Gaussian approximation itself is incorrect,[41] we prefer to follow the more rigorous method described in Warren's textbook.[41] Although this method is very expensive in terms of computer time, it is better suited to perform a detailed deconvolution of the total RDF.

Following Warren's method we can obtain a theoretical expression for the RDF in terms of N_{ij}, r_{ij}, and σ_{ij}, which are, respectively, the number of j-type neighbors, distance, and standard deviation of distance for the ij pair,

$$J_{\text{theor}}(r)=\sum_{i,j}x_iN_{ij}\frac{rP_{ij}(r)}{r_{ij}}\ , \tag{4}$$

where $P_{ij}(r)$ is a pair function defined as

$$P_{ij}(r)=\int_0^{q_{\max}} \frac{f_i f_j}{f_e^2} e^{-\alpha_{ij}^2 q^2} \sin(qr_{ij}) \sin(qr) dq \ , \quad (5)$$

where $\alpha_{ij}^2=\sigma_{ij}^2/2-\alpha^2$ involves the mean square relative displacement between atomic pairs σ_{ij}^2 and the width of the Gaussian window function α^2. To obtain the best fit we used the MINUIT subroutine of the CERN library to minimize the mean-square difference $\langle (J_{\text{theor}}-J_{\text{exp}})^2 \rangle$; the fitting parameters are N, r, and σ for each shell.

To avoid local minima in the fitting procedure and to reduce computer time, theoretical starting functions near the final ones are needed. We used a successive approximation scheme to fit experimental data. As a first step we fitted the first shell only using a small "r" range. In the second step first and second shells were fitted, but second shell starting parameters were calculated from the first-shell data of the preceding step. In the final step third shell contributions were included. Some of the third-shell peaks were near and below those of the second shell, so it was necessary to take them into account for a precise determination of disorder factors and coordination numbers. With the aim of avoiding the introduction of extra free parameters in the best-fit procedures, all third-shell parameters (area, disorder factors, and positions) were obtained from the data relative to the first two shells. Third neighbor contributions were simulated using the treatment by Paul, Connell, and Temkin,[50] which consists in the calculation of the third-neighbor distribution function from bond lengths and bond angles using a suitable form for the corresponding dihedral angle distribution function; to take into account the effects of bond length and bond angle distortions, it was convoluted with a Gaussian function. In the present analysis we used a flat dihedral angle distribution; the possibility of a nonflat distribution was tested; there was no significant change while number of fitting parameters increased.

We notice that, due to the great difference in atomic scattering factor of Si, C, and H the possible i-j pairs contribute with very different weight to $i(q)$ and thus to the experimental RFD. In fact the total pair correlation function $G(r)$ can be written as a weighted sum of partial pair correlation functions g_{ij},

$$G(r)=\frac{N}{2}\sum_{i,j} K_{ij} g_{ij}(r) \ , \quad (6)$$

where N is a normalization constant. Using a rough estimate,[41] the weight functions K_{ij} can be written

$$K_{ij} \approx x_i x_j f_i(0) f_j(0) \ , \quad (7)$$

so that they depend on the relative concentration x_i and on the atomic scattering factors at $q=0$. In a-$Si_{1-x}C_x$:H alloys there are in principle six PCF's $g_{ij}(r)$. The weight functions K_{ij} ensure that pair contributions involving H are negligible in all samples. In Si-rich samples, the weight function for C-C pairs is small compared to Si-Si pairs (e.g., for sample 2 we have $K_{CC}/K_{SiSi} \approx 0.01$) while at higher C concentrations Si-Si, C-C, and Si-C pairs have similar weights. The most important effect is that in Si-rich samples it is difficult to directly reveal the C-C contribution to the RDF. On the other hand, we are extremely sensitive to a small number of Si-Si bonds in C-rich samples (e.g., for sample 5 we have $K_{CC}/K_{SiSi} \approx 15$).

IV. RESULTS: DETAILED LOCAL STRUCTURAL DETERMINATION FOR Si AND C ATOMS

Before continuing we summarize the symbols used. We shall indicate a first-shell configuration with the symbol i-j, which means correlation between atoms i and j directly bonded, and second-shell configurations with the symbol i-$j(k)$, which means correlation between atoms i and j with atom k as a center. We shall indicate the first-shell parameters for the i-j pair with the symbol Φ_{ij} (with $\Phi=r,\sigma,N$) and the second-shell parameters for the i-$j(k)$ configuration with the symbol Φ_{ijk} (with $\Phi=r,\sigma,N,\theta$). We shall study two aspects of the atomic structure: the geometrical properties and chemical ordering. Bond lengths, bond angles, and disorder factors define geometrical disorder and local structural symmetries. Chemical ordering concerns the coordination number of each site and the distribution of bond types in the alloy. For the first neighbors, as already remarked, bond-type distribution varies between two extreme situations: complete random order and complete chemical order. In the RO case the distribution of bonds is purely statistical and completely determined by atomic coordinations and relative concentrations. For an $A_{1-x}B_x$ alloy RO is characterized by the presence of A-A, B-B, and A-B bonds for all compositions other than $x=0$ and 1. In the opposite case of CO, heteronuclear bonds A-B are maximized at all concentrations. In this case there exists a stoichiometric concentration x_c at which only A-B bonds exist. At concentrations other than x_c only homonuclear bonds for the majority element can exist. For the next-nearest-neighbor configurations there are three extreme cases: the RO case, for which all i-$j(k)$ configurations can exist with a random distribution, and two kinds of CO, CO with homogeneous dispersion (COHD) and CO with phase separation (COPS). For an $A_{1-x}B_x$ alloy COHD represents the situation in which the bonds allowed by CO are homogeneously dispersed in the alloy, so that for A-rich samples we can find A-$A(A)$, A-$B(A)$, A-$A(B)$, and B-$B(A)$ configurations; on the other hand, in COPS, "mixed" configurations such as A-$B(A)$ are not present[11] and the material consists of two microphases: a pure A phase and a chemically ordered AB alloy phase.

The results of our analysis are presented in Figs. 1–8. In Fig. 1, on the left-hand side, the experimental data and the total RDF's of the five samples studied are shown. The behavior of the structure function reveals the modifications induced by C inclusion: as x increases its amplitude decreases due to the smaller scattering factor of C compared to Si and the frequency changes due to the presence of different distances. The short-range order modifications are better highlighted in the RDF plots. It should be kept in mind that the relative magnitude of the different peaks is severely affected by the scattering factors of the pair involved. Qualitatively speaking, the RDF's show the gradual growth of the C-C peak at ≈ 1.5

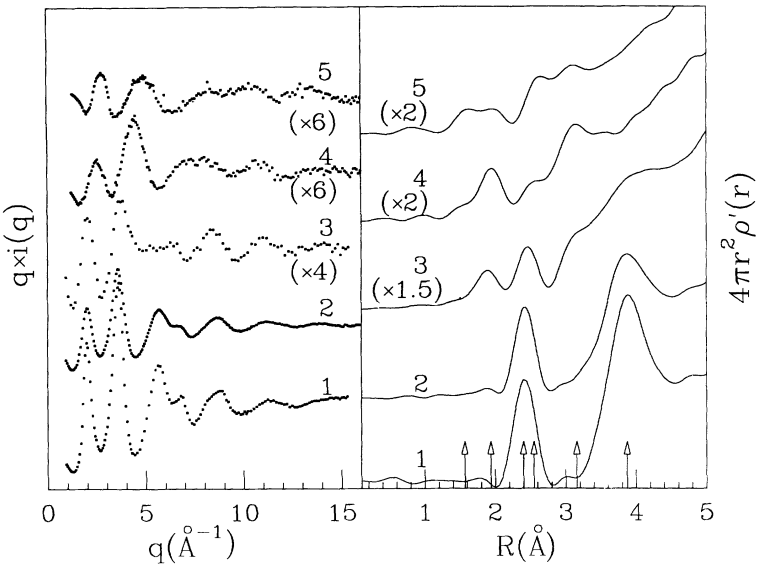

FIG. 1. Left panel: experimental structure factors. Right panel: total radial distribution functions. Arrows in right panel indicate nearest- and next-nearest-neighbor distances in crystals.

Å, while the Si-C peak, at ≈ 1.86 Å, has its maximum value for intermediate concentrations, and the Si-Si peak at ≈ 2.36 Å vanishes in C-Rich samples, leaving an evident minimum between first- and second-shell configurations. Second-shell contributions, which are well defined in Si-rich samples, gradually become more closely spaced as x increases. The Si-Si(Si) peak, at ≈ 3.85 Å, vanishes in C-rich samples, leaving a smooth feature deriving from higher-shell configurations; the Si-Si(C) and C-C(Si) peaks, at ≈ 3.12 Å, and C-C(C), at ≈ 2.50 Å, are clearly visible in C-rich samples.

In Fig. 2 two examples of the fits for the total RDF's, for samples 2 and 4, are given. These examples illustrate the behavior we have found also for the remaining samples. In fact, in the first shell no minority homonuclear bonds have been found (this is especially significant for high x, since there is a high sensitivity to Si-Si bonds in this concentration region) and the types of second-shell contributions differ for large and small x: at low C content all second-shell configurations compatible with the first shell are detected while at high C content no mixed configuration C-Si(C) is found.

In Fig. 3 the interatomic distances obtained for the first- and second-shell configurations are presented; the interatomic distances found in diamond, graphite, Si, and SiC (all in the crystalline form) are plotted as dotted lines. Clearly the interatomic distances in the first and second shell are close to those of the crystal and are independent from x (no significant trend is observed). The C-C distances, both in the first and second shells, are between those expected for graphitic and sp^3 configurations, consistent with a mixture of sp^2 and sp^3 hybridized C. First- and second-shell distances agree with previous determinations.[51] The Si-Si peak is located at 2.36 ± 0.005 Å in samples 1 and 2, while it exhibits a small increase to 2.39 Å in sample 3. This is surprising given the general finding of constant bond lengths in amorphous semiconductors[2] and the EXAFS measurements[6] in which this distance was found constant at 2.35 ± 0.01 Å. We believe that it is an artifact due to the presence of a weak, un-

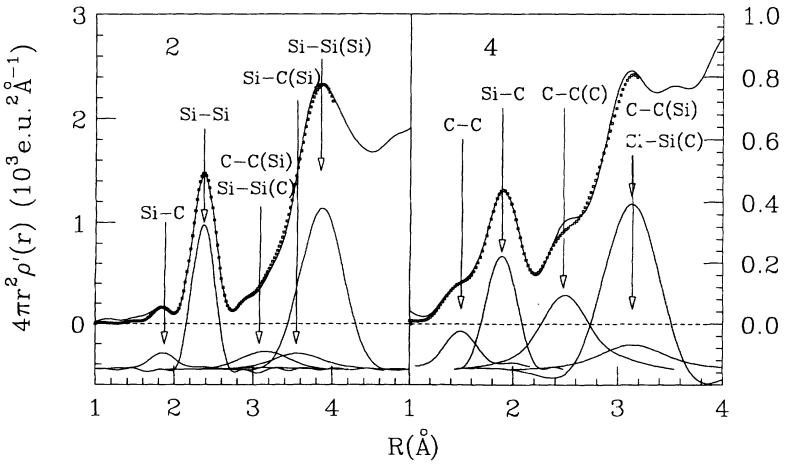

FIG. 2. Examples of best fits for samples 2 and 4. The data are shown as a continuous line, the fit as points. Also shown are individual peak contributions. e.u. stands for electronic units.

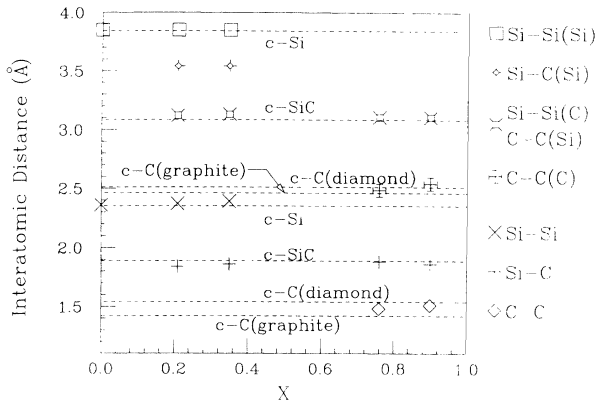

FIG. 3. Interatomic distances of all nearest- and next-nearest-neighbor configurations.

resolved, second-shell C-C(C) peak. Such a contribution can distort the main Si-Si peak since the second-shell distances in graphite and diamond, 2.46 and 2.51 Å, respectively, are near the Si-Si first-shell peak. We have tested this possibility by adding a C-C(C) peak at ≈ 2.46 Å in the fit: as a result the Si-Si peak shifted to a lower bond length. In spite of this, because of the poor sensitivity to C-C scattering in Si-rich samples, quantitative results are uncertain and we prefer not to use this correction in order to avoid introducing more parameters. On the other hand, this is in qualitative agreement with the existence of a small quantity of homonuclear C-C bonds below $x=0.5$. We observe that for the two C-rich samples the second shell is fitted well without any Si-C(C) contributions for which we have a greater sensitivity than for C-C(C) due to its higher weight function. This means that C-C and C-C(C) configurations, if any, must come from a separated carbon phase, polymeric or graphitic, rather than dispersed in the network.

The $\sigma^2_{SiSi}(r)$ value (Fig. 4) is equal to 5.5×10^{-3} Å^2 in a-Si:H, in agreement with previous determinations,[51] and increases to 6.4×10^{-3} Å^2 in the alloy samples. The $\sigma^2_{CC}(r)$ values are about 1.5 times greater[52] than pure a-C and they are about twice $\sigma^2_{SiSi}(r)$. These high values are unusual because[22] the C-C bonds are stronger than Si-Si and we expect that the former would be more ordered than the latter. A contribution to this fact is undoubtedly that the C-C peak width comes from the two unresolved peaks of sp^2 and sp^3 configurations rather than from a continuous bond distribution.

Comparing the $\sigma^2(r)$ values obtained for the first and second shells we observe that whereas σ^2_{CC} is equal to or higher than others in the first shell, it is smaller in the second shell. This must be explained, at least in part, by the fact that the static disorder observed in the first and second shells around C comes from two different effects: in the first shell the disorder factor is dominated by the peak separation ($\Delta r\approx0.12$ Å) while in the second shell the two configuration distances are closer ($\Delta r\approx0.05$ Å) and the width of the RDF peak is essentially due to the true disorder factor.

In Fig. 5 the bond angles, as deduced from the first- and second-shell bond lengths, are plotted. θ_{SiSiSi} is always close to the tetrahedral value of 109.47°; the slightly lower value of this quantity for sample 2 is due to the erroneous determination of the first-shell bond length, as discussed above. The C-C(C) bond angle is found at $113.6°\pm0.2°$, which is between the values expected for sp^2 and sp^3configurations. The bond angle value obtained Si-C(Si) is higher than tetrahedral at $\approx113°$; this suggests that bond bending forces are weaker on Si sites with a mixed first shell and that the inclusion of C in the a-Si:H leads to an increase of this angle. Also reported is the contribution from Si-Si(C) and C-C(Si) configurations. We expect a small difference between C-centered and Si-centered configurations due to the coexistence of sp^2 and sp^3 C hybridizations whereas Si atoms are expected only in sp^3 configurations; however, we have not resolved these two situations to reduce the number of free parameters in the fitting procedure. In Si-rich samples the Si scattering factors exalts the Si-Si(C) weight factor and the angle is consistent with partial graphitic hybridization of the central atom. On the other hand, as x increases the

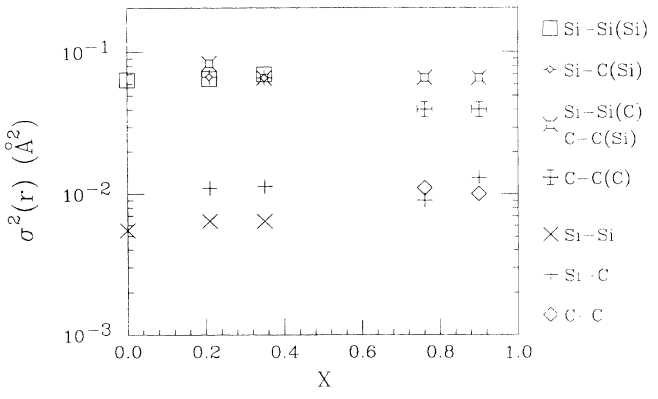

FIG. 4. Mean-square relative displacements for all interatomic distances measured.

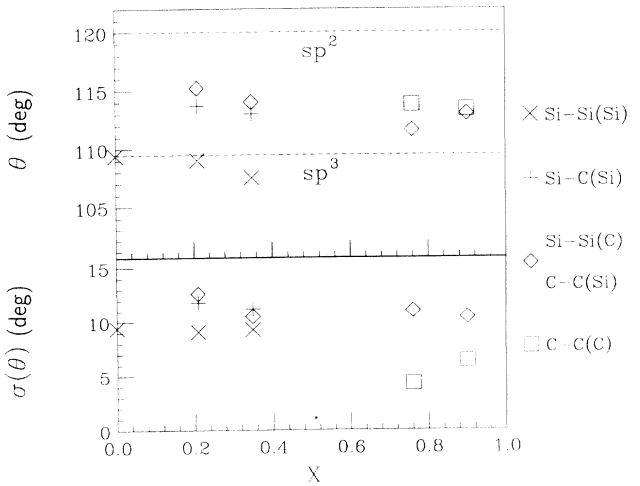

FIG. 5. Bond angles and their fluctuation, as deduced from the interatomic distance measurements.

weight of C-C(Si) arrangements increases and thus the bond angle decreases since only tetrahedral arrangement of Si sites are present. The presence of a partial graphitic hybridization is compatible also with our previous EXAFS data.[6]

From the $\sigma^2(r)$ and θ values we have calculated the fluctuation of the bond angle for a i-$j(k)$ configuration, by using

$$\sigma(\theta)=\frac{r_{ijk}\sigma_{ijk}(r)-|r_{ik}-r_{jk}\cos(\theta)|\sigma_{ik}(r)-|r_{jk}-r_{ik}\cos(\theta)|\sigma_{jk}(r)}{|r_{jk}r_{ik}\sin(\theta)|} . \quad (8)$$

The $\sigma(\theta)$ values obtained, which are reported in the bottom half of Fig. 5, are all in the range 5°–15°, compatible with the fact that in amorphous semiconductors bond angle fluctuations are of the order of 10% of the angle mean value. The angular disorder obtained ($\approx 4°$) agrees with results[52] on a-C.

In Fig. 6 we show the mean coordination numbers for Si and C and the mean total coordination number $N=(1-x)N_{Si}+xN_C$. N_{Si} is obtained from $N_{Si}=N_{SiC}+N_{SiSi}$ and similarly for N_C. H inclusion reduces the observed coordination number because its scattering amplitude is negligible, so C-H and Si-H bonds are invisible in x-ray diffraction data. By using $N_{SiSi}=4-x_H/(1-x_H)$, the hydrogen concentration x_H for the a-Si:H sample is found to be $\approx 23\%$. A similar calculation cannot be done for alloy samples because we do not have an independent measurement of the relative fraction of sp, sp^2, and sp^3 C.

The continuous decrease of the mean coordination number with x agrees with the experimental evidence that as the C concentration increases, H inclusion and the fraction of sp^2 bonded C also increase. This fact is in agreement with the decrease in the bulk density, the values of which are reported in Table I and agree with the literature data for a-Si:H (Ref. 51) and a-C:H.[53] Si exhibits a mean coordination number which is always between 3.4 and 3.7 and is always higher than N_C: this agrees with the evidence[13] that H is preferably bonded to C. We notice that at intermediate concentration N_{Si} presents a weak minimum. This is most probably due to the fact[1,22] that Si-C bonding induces an increase in Si-H bond strength compared to C-H. At intermediate compositions, in which Si-C bonds are maximized, the number of H atoms bonded to Si is thus greatest.

In sample 2 the value of $N_C=2.2$, obtained from the Si-C peak area, is very small. A small value for N_C has also been inferred by EXAFS analysis[6] where the data on a sample with $x=0.26$ was consistent with $N_C\approx 2$. Infrared spectra,[15,16] as well as mass density measurements,[54] show that, depending on deposition conditions, C can be incorporated mainly as methyl groups and estimate that the C-H bond content is up to 33% of the total C bonds,[14,15] which would lead to $N_C=2.7$. We believe that the value found in the present analysis could, at least in part, be due to the fact that some C is found in a Si-free phase and that the resulting C-C bonds are undetected in XRS due to the low weight of such configurations. In fact, in this case, the extra C-C bonds would raise N_C to a value closer to 3. The reduced growth temperature of the present samples might enhance the volume fraction of the Si-free phase.[14] On the other hand, we point out that the coordination numbers reported in Fig. 6 were calculated using the total C concentrations obtained by SNMS. Given that we are poorly sensitive to the Si-free phase, the correct value of N_C for the SiC alloy phase should be obtained by using the C concentration in this

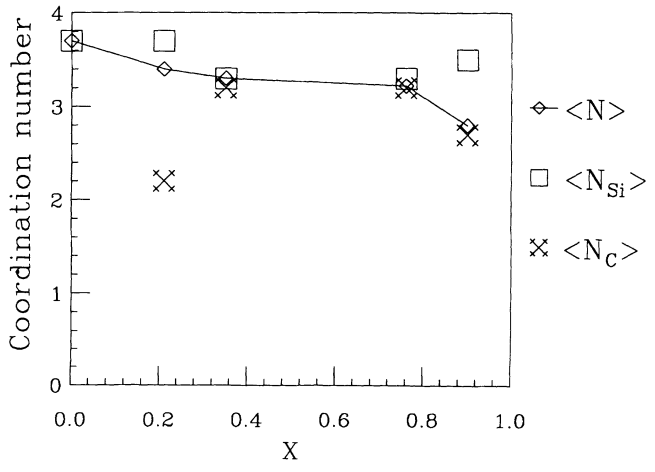

FIG. 6. Mean coordination numbers for Si and C atoms and the mean total coordination number.

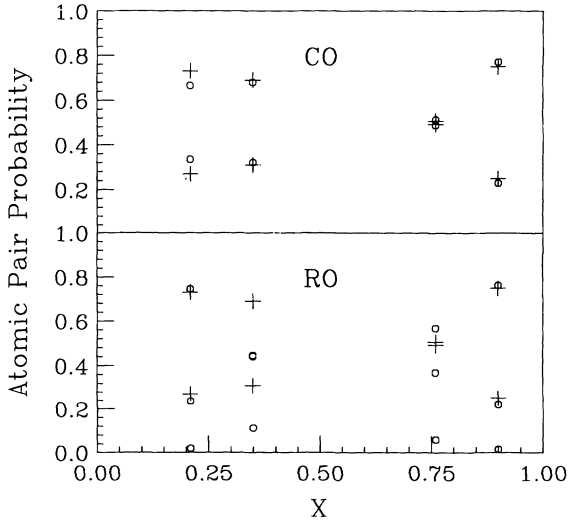

FIG. 7. Experimental first-shell atomic pair probabilities (crosses) compared to those predicted in the CO and RO hypotheses (open circles).

phase, which is certainly less than the total. This would contribute to the increase in N_C. In fact, as it can be seen from Eq. (4), the coordination number obtained by a fit of a $J_{exp}(r)$ peak is inversely proportional to the concentration used.

We present in Fig. 7 the plots of the normalized first-shell coordination numbers as a function of x, compared to the expected values assuming either complete CO or complete RO. In Fig. 8 a similar plot for the second shell is shown together with expected values assuming COPS or COHD, respectively. Since mean coordination numbers for Si and C are different (and not equal to 4), comparing the experimental results with a theoretical plot obtained using a stoichiometric concentration of 0.5 can be misleading. Thus theoretical value reported in Figs. 7 and 8 were obtained using the experimental coordination numbers (Fig. 6) as the effective valence for Si and C. In this way we were able to take into account the effect of H inclusion and C hybridizations other than sp^3. As for the first shell, the data clearly fit the CO hypothesis better than RO. Due to the different weights of the contributions it is much easier to estimate the number of minority homonuclear bonds in C-rich samples than in Si-rich samples. In particular we stress that in RO a significant Si-Si contribution, 0.06 normalized bonds per Si atom, is predicted for sample 4. This has not been detected, notwithstanding a high sensitivity to such a contribution; more precisely we estimate that the maximum number of Si-Si bonds per Si atom compatible with the data is 0.02. In the second shell it is quite clear that COPS provides the best fit with experimental data for C-rich samples while for Si-rich samples agreement seems to be best with COHD for sample 2 and no satisfactory fit is found for sample 3. In order to clarify the situation at high C concentration in Fig. 9 we compare our fit (left panel) with a hypothetical RDF (right panel) in which the first-shell parameters have been used to calculate the second-shell contribution in the COHD hypothesis. We observe that

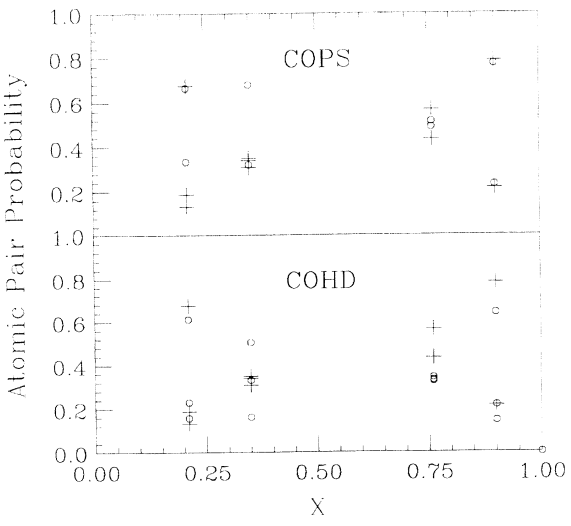

FIG. 8. Experimental second-shell atomic pair probabilities (crosses) compared to those predicted in the COPS and COHD hypotheses (open circles).

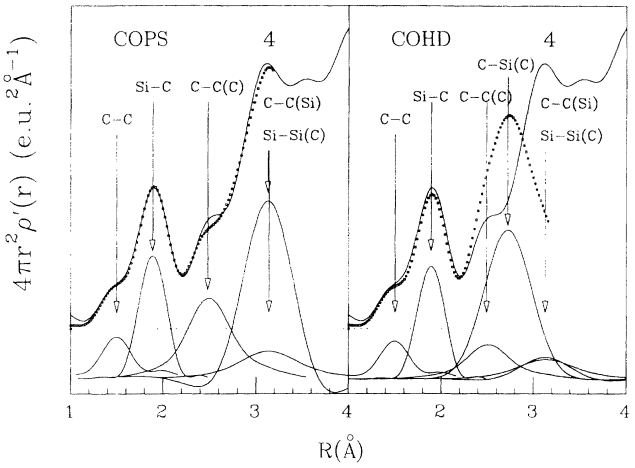

FIG. 9. Left panel: experimental data (continuous line) and best fit (dots) for sample 4. Right panel: same as in the left panel but with a hypothetical RDF built by using the first-shell coordination numbers in the COHD hypothesis.

the Si-Si(C) and C-C(Si) contributions become very small, while the big peak of the Si-C(C) configuration appears at ≈ 2.7 Å; the result is a very poor comparison with experimental data. A similar analysis can be performed for sample 5. The conclusion is that in C-rich samples chemical order is of the certainly of the COPS type. In Si-rich samples the situation is less clear, with a good fit to COHD at low x. A similar trend has been pointed out in the literature.[8,11]

V. DISCUSSION: BOND LENGTHS AND DEGREE OF CHEMICAL ORDERING

After having provided a detailed picture of local bonding we now discuss two important question on the structure of a-$Si_{1-x}C_x$:H: the behavior of bond lengths and the degree of chemical ordering.

The evidence provided clearly indicates that all bond lengths in first and second shell are close to the crystalline value and do not vary in a significant way with x. The present result confirms the general trend found using EXAFS in a wide class of amorphous alloys[2] and extends it to include next-nearest neighbors. This implies that although bond angles have a 10% static fluctuation, their mean values remain unchanged so that the elementary tetrahedral and graphitic units can be considered as building blocks of the material, notwithstanding the presence of many phases at the microscopic level and the absence of long range order.

The present situation must be compared with what occurs in crystalline semiconductor alloys. In fact in pseudobinary alloys of the type $In_{1-x}Ga_xAs$ it has been found[33] that, whereas the lattice constant varies linearly with x following Vegard's law, the individual bond lengths exhibit a smaller (but nonzero) variation, with a tendency to remain close to their "natural value." This only apparently contradicts the requirement of long-range order: in the model proposed[55] for $Cd_{1-x}Mn_xTe$

the cations remain fixed on their lattice positions while the anion moves from its ideal position in order to minimize the strain energy and keep the bond lengths as near as possible to their natural value.

These ideas have been put on a firm ground by two theoretical approaches, which successfully reproduce the experimental data on a wide class of material.[35-37,39] In the framework of a Keating interatomic potential it is shown that the relative magnitude of bond stretching (α) and bond bending (β) force constants determines to what extent the bond lengths exhibit variations with composition: for weak angular force constants the lattice is "floppy" and there are only weak variations of the bond lengths while large angular forces lead to a rigid lattice in which bond lengths are forced to follow more closely the variation of the lattice parameter.

Mousseau and Thorpe have studied the effect of amorphicity on bond length variation for the case of SiGe alloys and have found that the loss of long-range order does not significantly change the predicted variations. Hence we believe it is useful to compare the expected variation of bond lengths in crystalline $Si_{1-x}C_x$ alloys with the present experiments. In Fig. 10 we report as the solid lines the theoretical variation according to Cai and Thorpe, with the ratio β/α taken from Martin[56] (for the SiC bond length Martins and Zunger predict a similar overall variation but with a downward shift of 0.15 Å). The points represent the experimental measurement taken from the present data and from the EXAFS determination.[6] Note that in the present case static bond length fluctuations amount to, at most, ~0.1 Å, so that they cannot obscure the 0.4 Å variation expected. There is no doubt that the expected variations in bond length in crystalline $Si_{1-x}C_x$ are not detected in a-$Si_{1-x}C_x$:H. There can be a number of reasons for this. First, the theoretical estimate does not take into account graphitic and/or polymeric C bonding, which can alter the value of angular force constants. Second, the effect of H is also important in making the network less rigid and has been used by Mousseau and Thorpe[39] to explain (at least in part) the lack of variation in bond length in a-$Si_{1-x}Ge_x$:H. Finally, it is possible that the lack of long-range order does in fact make the network more floppy than in the crystalline case.

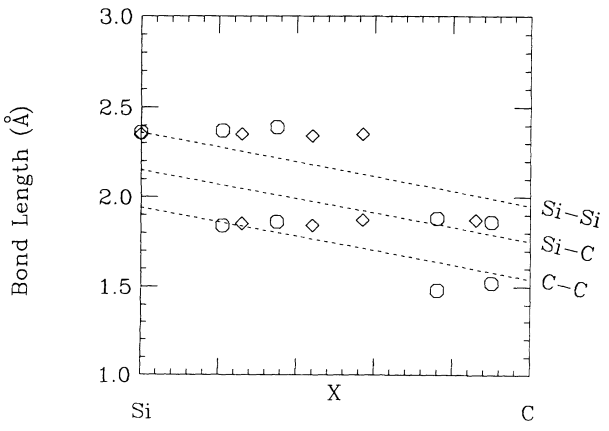

FIG. 10. Comparison of the predicted variation of nearest-neighbor bond lengths in crystalline SiC with the experimental data from the present work (circles) and EXAFS (diamonds).

We now comment on the degree of chemical ordering present in a-$Si_{1-x}C_x$:H. As explained in Sec. IV, the present experimental evidence points to a strong tendency for chemical order, as borne out by the nearest-neighbor coordination numbers and confirmed by EXAFS as far as the Si environment is concerned. Furthermore, it agrees with other experimental evidences, as briefly reviewed in Ref. 3. For C-rich samples the chemical order is found to be of the COPS type, while at low x the situation is less clear. This tendency for chemical order should not be over interpreted, as it is clear that polymeric and graphitic C do exist. The problem of chemical ordering in semiconductor alloys has been addressed in both crystalline[38] and amorphous[28,40] systems. In crystals the enthalpy of mixing can be divided in two parts: a chemical term deriving from charge transfer and a strain term deriving from bond deformation. Using this approach the authors found in Si-Ge alloys a tendency against chemical ordering while in Si-C alloys a strong preference for heterobonds is predicted. Smith and Yin, using an approach that is more appropriate for amorphous materials which also includes bonding to H, minimized the free energy, thus taking into account entropy effects. A large amount of chemical order is predicted for a-$Si_{1-x}C_x$:H, in agreement with the present results.

We consider it useful, at this point, to compare our results with recent theoretical models of amorphous silicon-carbon alloys. We will look at three recent models: a continuous random network[57] (CRN) model, an *ab initio* molecular-dynamics (MD) model,[24] and free-energy model[22,28,40] (FEM) obtained from a statistical thermodynamics approach.

The CRN models were the first models used to simulate the structure of amorphous covalent materials.[58-60] Energy minimization of a disordered starting structure is achieved by a Monte Carlo algorithm using a simple expression for the interatomic potential. The CRN model proposed by Kelires[25] for a-$Si_{1-x}C_x$:H uses empirical potentials,[61] already tested with good results on a-Si,[57] a-C,[62] and c-SiC.[61] Although C-C homonuclear bonds are observed in Si-rich samples, this model presents a high degree of CO in agreement with our results; the first-shell composition of the model with $x=0.5$ suggests that C atoms in chemically ordered environment are sp^3 hybridized.

MD simulations with interatomic potentials obtained from first principles have recently received much interest. Most of the recent progress is due to the approach introduced by 1985 by Car and Parrinello.[63] Excellent results have been obtained in a large variety of systems such as a-Si (Ref. 64) and a-C.[65] In spite of this, the model built for a stoichiometric a-SiC sample yields a geometrically high distorted structure and a high degree of chemical disorder, in disagreement with the present findings. This high degree of disorder can be partially due to the absence of hydrogen in the model, which would confirm the role of H inclusion in promoting chemical order. We point out that the model does not reproduce other experi-

mental features such as the electronic density of states.[4]

The FEM (Refs. 28 and 22) for bonding in amorphous covalent alloys is based on the quasichemical approach to the thermodynamics of regular solutions.[66] The normalized bond concentrations are obtained minimizing the Gibbs free energy. Samples with different relative concentrations of Si and C are simulated at high and low H concentrations. At high H concentration essentially all C and H atoms enter as CH_3 units leading to a "methylated amorphous silicon structure" a-$Si_{1-x}(CH_3)_x$:H and only one Si-C bond per C atom is predicted. As previously mentioned the observed correlation between the increase in Si-H and Si-C bonding predicted by this model is confirmed by our data and borne out by the shallow minimum of N_{Si} at intermediate concentrations. The FEM predicts a strong tendency for chemical order, with some residual entropy effects, and is thus confirmed by our measurements.

ACKNOWLEDGMENT

We are very grateful to Dr. Moro (Istituto Ricerca Scientifca e Tecnologica, Trento, Italy) for the SNMS concentration measurements.

[1]J. Bullot and M. P. Schmidt, Phys. Status Solidi B **143**, 145 (1987).
[2]F. Boscherini, in *Amorphous Silicon Technology—1992,* edited by M. J. Thompson, Y. Hamakawa, P. G. LeComber, A. Madan, and E. A. Schiff, MRS Symposia Proceedings No. 258 (Materials Research Society, Pittsburgh, 1992), p. 217.
[3]F. Evangelisti, J. Non-Cryst. Solids **164&165**, 1009 (1993).
[4]M. De Seta, S. L. Wang, F. Fumi, and F. Evangelisti, Phys. Rev. B **47**, 7041 (1993).
[5]T. M. Burke, P. J. R. Honeybone, D. W. Huxley, R. J. Newport, Th. Frauenheim, P. Blaudeck, and Th. Kohler, in *Novel Forms of Carbon,* edited by C. L Renschler, J. J. Pouch, and D. M. Cox, MRS Symposia Proceedings No. 270 (Materials Research Society, Pittsburgh, 1992), p. 97.
[6]S. Pascarelli, F. Boscherini, S. Mobilio, and F. Evangelisti, Phys. Rev. B **45**, 1650 (1992).
[7]C. Meneghini, S. Pascarelli, F. Boscherini, S. Mobilio, and F. Evangelisti, J. Non-Cryst. Solids **75**, 137 (1991).
[8]M. De Seta, P. Narducci, and F. Evangelisti, in *Amorphous Silicon Technology—1991,* edited by A. Madan, Y. Hamakawa, M. Thompson, P. C. Taylor, and P. G. LeComber, MRS Symposia Proceedings No. 219 (Materials Research Society, Pittsburgh, 1991), p. 265.
[9]R. C. Fang and L. Ley, Phys. Rev. B **40**, 3818 (1989).
[10]H.-K. Tsai, W.-L. Lin, W. J. Sah, and S.-C. Lee, J. Appl. Phys. **64**, 1910 (1988).
[11]D. R. McKenzie, G. B. Smith, and Z. Q. Liu, Phys. Rev. B **37**, 8875 (1988).
[12]D. L. Williamson, A. H. Mahan, B. P. Nelson, and R. S. Crandall, in *Amorphous and Crystalline Silicon Carbide II,* edited by M. M. Rahman, C. Y. W. Yang, and G. L. Harris, Springer Proceedings in Physics Vol. 43 (Springer-Verlag, Berlin, 1989), p. 89.
[13]E. Kaloyeros, R. B. Rizk, and J. B. Woodhouse, Phys. Rev. B **38**, 13 099 (1988).
[14]M.A. Petrich, K. K. Gleason, and J. A. Reimer, Phys. Rev. B **36**, 9722 (1987).
[15]K. Mui, D. K. Basa, F. W. Smith, and R. Cordeman, Phys. Rev. B **8089**, (1987).
[16]A. H. Mahan, B. von Roedern, D. L. Williamson, and A. Madan, J. Appl. Phys. **57**, 8 (1984).
[17]Y. Inoue, S. Nakashima, A. Mitsuishi, S. Tabata, and S. Tsuboi, Solid State Commun. **48**, 1071 (1983).
[18]Y. Katayama, K. Usami, and T. Shimada, Philos. Mag. B **43**, 283 (1981).
[19]W. Y. Lee, J. Appl. Phys. **31**, 3365 (1980).
[20]H. Wieder, M. Cardona, and C. R. Guarnieri, Phys. Status Solidi B **92**, 99 (1979).
[21]M. Gorman and S. A. Solin, Solid State Commun. **15**, 761 (1974).
[22]H. Efstathiadis, Z. Yin, and F. W. Smith, Phys. Rev. B **46**, 13 119 (1992).
[23]J. Robertson, Philos. Mag. B **66**, 615 (1992).
[24]F. Finocchi, G. Galli, M. Parrinello, and C. M. Bertoni, Phys. Rev. Lett. **68**, 3043 (1992).
[25]P. C. Kelires, Europhys. Lett. **14**, 43 (1991).
[26]F. Finocchi, G. Galli, M. Parrinello, and C. M. Bertoni, J. Non-Cryst. Solids. **137&138**, 153 (1991).
[27]K. Mui and F. W. Smith, Phys. Rev. B **35**, 8080 (1987).
[28]Z. Yin and F. W. Smith, Phys. Rev. B **43**, 4507 (1991).
[29]A. Filipponi, P. Fiorini, F. Evangelisti, and S. Mobilio, in *Amorphous Silicon Semiconductors—Pure and Hydrogenated,* edited by A. Madan, M. Thompson, D. Adler, and Y. Hamakawa, MRS Symposia Proceedings No. 95 (Materials Research Society, Pittsburgh, 1987), p. 305.
[30]L. Incoccia, S. Mobilio, M. G. Proietti, P. Fiorini, C. Giovannella, and F. Evangelisti, Phys. Rev. B **31**, 1028 (1985).
[31]F. Boscherini, A. Filipponi, S. Pascarelli, F. Evangelisti, S. Mobilio, F. C. Merques, and I. Chambouleyron, Phys. Rev. B **39**, 8364 (1989).
[32]S. Pascarelli, F. Boscherini, S. Mobilio, A. R. Zanatta, F. C. Marques, and I. Chambouleyron, Phys. Rev. B **46**, 6718 (1992).
[33]J. C. Mikkelsen, Jr. and J. B. Boyce, Phys. Rev. Lett. **49**, 1412 (1982).
[34]J. C. Mikkelsen, Jr. and J. B. Boyce, Phys. Rev. B **28**, 7130 (1983).
[35]Y. Cai and M. F. Thorpe, Phys. Rev. B **46**, 15 872 (1992); **46**, 15 879 (1992).
[36]J. L. Martins and A. Zunger, Phys. Rev. B **30**, 6217 (1984).
[37]N. Mousseau and M. F. Thorpe, Phys. Rev. B **48**, 5172 (1992).
[38]J. L. Martins and A. Zunger, Phys. Rev. Lett. **56**, 1400 (1984).
[39]N. Mousseau and M. F. Thorpe, Phys. Rev. B **46**, 15 887 (1992).
[40]F. W. Smith and Z. Yin, J. Non-Cryst. Solids **137&138**, 871 (1991).
[41]B. E. Waren, *X-Ray Diffraction* (Addison-Wesley, Reading, MA, 1969).
[42]H. P. Klug and L. E. Alexander, *X-Ray Diffraction Procedures for Polycrystalline and Amorphous Materials* (Wiley, New York, 1974).
[43]B. D. Cullity, *Elements of X-Ray Diffraction* (Addison-Wesley, Reading, MA, 1978).
[44]M. Magini, G. Licheri, G. Piccaluga, G. Pascina, and G. Pinna, *X-Ray Diffraction of Ions in Aqueous Solutions* (CRC, Boca Raton, FL, 1988).

[45]R. Jede, H. Peters, G. Dunnebier, O. Ganschow, U. Kaiser, and K. Seifert, J. Vac. Sci. Technol. A **6**, 2271 (1988).
[46]H. C. Macgillavry and G. D. Rieck, *International Tables for X-Ray Crystallography,* 2nd ed. (Kynoch, Birmingham, England, 1968), Vol. III.
[47]C. W. Dwiggins, Jr., Acta Crystallogr. Sect. A **28**, 155 (1972).
[48]J. Krog-Moe, Acta Crystallogr. **9**, 951 (1956).
[49]N. Normam, Acta Crystallogr. **10**, 370 (1957).
[50]W. Paul, G. A. N. Connell, and R. J. Temkin, Adv. Phys. **22**, 531 (1973).
[51]W. Shulke, Philos. Mag. B **43**, 451 (1981).
[52]F. Li and J. Lannin, Phys. Rev. Lett. **65**, 1905 (1990).
[53]J. Robertson, Adv. Phys. **35**, 317 (1986).
[54]J. Sotiropulos and G. Weiser, J. Non-Cryst. Solids **97&98**, 1088 (1987).
[55]A. Balzarotti, M. Czyzyk, N. Motta, M. Podgorny, and M. Zimnal-Starnawska, Phys. Rev. B **30**, 2295 (1984).
[56]R. M. Martin, Phys. Rev. B **1**, 1005 (1970).
[57]P. C. Kelires and J. Tersoff, Phys. Rev. Lett. **61**, 562 (1988).
[58]D. E. Polk, J. Non-Cryst. Solids **5**, 365 (1971).
[59]F. Wooten, K. Winer, and D. Weaire, Phys. Rev. Lett. **54**, 1392 (1985).
[60]F. Wooten and D. Weaire, Solid State Phys. **40**, 1 (1987).
[61]J. Tersoff, Phys. Rev. B **39**, 5566 (1989).
[62]J. Tersoff, Phys. Rev. Lett. **61**, 1164 (1988).
[63]R. Car and M. Parrinello, Phys. Rev. Lett. **55**, 2471 (1985).
[64]R. Car and M. Parrinello, Phys. Rev. Lett. **60**, 204 (1988).
[65]G. Galli, R. M. Martin, R. Car, and M. Parrinello, Phys. Rev. Lett. **62**, 555 (1989).
[66]P. Gordon, *Principle of Phase Diagrams in Materials Systems* (McGraw-Hill, New York, 1968).